

OPTICAL CONTROL AND TUNING OF THERMAL-PIEZORESISTIVE SELF-SUSTAINED OSCILLATORS

Harris J. Hall¹, Luda Wang¹, J. Scott Bunch¹, Siavash Pourkamali², and Victor M. Bright¹

¹University of Colorado, Boulder, USA

²University of Texas, Dallas, USA

ABSTRACT

The ability to frequency tune and provide on/off control of electrically driven thermal-piezoresistive self-sustained oscillators through the application of HeNe (632 nm wavelength) laser illumination to devices is reported in this work. Photoexcitation of charge carriers is presented as the physical mechanism to control the piezoresistive coefficient and electrical resistivity enabling these abilities. The results are significant in that they offer a novel means to directly control the electronic output of RF oscillators through photonics.

INTRODUCTION

Developing effective interconnect mechanisms between radio frequency (RF) and optical signals remains an area of interest to further leverage the benefits of optical communication and control between electronic devices. Micro and nanoscale mechanical resonators have played a central role in providing on-chip methods of integration between these two domains with the goal of realizing photonic integrated circuits in mind. Opto-mechanical resonators have gained considerable attention where suspended structures are deflected with nanoscale precision using the optical gradient force [1], actuated into oscillation with continuous wave laser illumination [2], and electrically actuated to modulate optical waveguides [3].

Thermally-actuated piezoresistively readout resonant devices fabricated from single-crystal silicon have gained interest in the RF MEMS community, particularly for their ability to exhibit self-sustained oscillation under DC bias [4]. Previous work, expanded their range of operation into the VHF regime [5] and applied their use towards a variety of sensing applications. In this work we show how the steady-state performance of these devices operating in self-sustained oscillation changes when under direct illumination of HeNe laser light. Specifically we demonstrate the ability to both frequency tune and provide on/off control of the oscillation by adjusting the laser power.

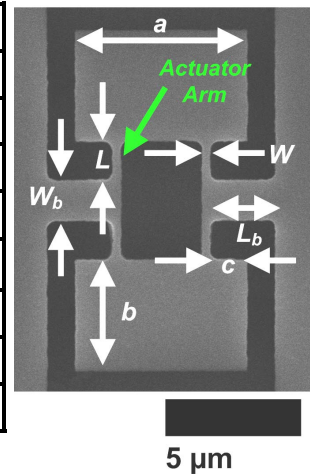
Device Background

The devices examined in this work are the same as presented in [5] which described their fabrication and performance (unilluminated and at fixed low laser power) as both resonators and self-sustained oscillators. The device dimensions and 2-terminal I-shaped geometry are shown in Table 1. These devices were intended to operate in the in-plane longitudinal structural mode through cyclic Joule heating of the actuator arms, however evidence presented in [5] suggested that the actual mechanical mode of operation

is likely of an alternate shape. The devices were fabricated from n-type (phosphorus doped) single crystal silicon ($\rho \sim 0.1 \Omega\text{-cm}$, $\sim 8.1 \times 10^{16} \text{ cm}^{-3}$ at 300K) using an SOI wafer (oxide layer $\sim 3 \mu\text{m}$) based process. The strong negative piezoresistive coefficient of this material enables the ability for self-sustained oscillation under constant DC bias through internal feedback [4].

Table 1: Top View of Device A3 with average device dimensions [$n=7$] in μm (h = device thickness)

Device	C6	A3
h	1.8	1.6
a	5.73	6.46
b	5.70	4.17
c	0.94	1.38
L	2.02	1.47
W	0.34	0.36
W_b	1.59	1.54
L_b	2.56	2.56



THEORY

The performance of these devices under photoillumination can be considered from the perspective of the device's motional conductance at resonance ($\omega = \omega_o$), g_m , defined in [6] as

$$g_m = 2\alpha E \pi_l Q_m \frac{I_{DC}^2}{C_{th} \omega_o} \quad (1)$$

where Q_m is mechanical quality factor, I_{DC} is the applied DC current, C_{th} is the effective thermal capacitance of the lumped actuator element, E is the Young's modulus, π_l is the longitudinal piezoresistive coefficient, and α is the coefficient of thermal expansion. It is critical to note that (1) is based upon a lumped model for the actuator arms at the center of the device. Thus it is the photon interaction that occurs locally to this area that is of primary interest. Of these parameters shown in (1) it can be expected that three of them may be affected by the HeNe illumination.

First, the resistivity of the silicon should decrease due to photoexcitation of carriers since the photon energy of HeNe laser light ($\sim 1.96 \text{ eV}$) exceeds both the extrinsic bandgap ($\sim 0.15 \text{ eV}$ at 300K) and the intrinsic bandgap of

silicon (~ 1.12 eV). Thus increasing illumination should increase the I_{DC} and alter the device power dissipation, depending upon how the device is biased. This will in turn alter the Joule heating occurring and change the steady-state temperature. It can also be expected that charge carriers pumped high above the conduction band minimum will relax via phonon scattering mechanisms causing additional heating of the material. Since the Young's modulus is temperature dependent it should thus change with HeNe laser illumination.

Finally, per the many-valleys model [7], the piezoresistive effect in n-type silicon is due to a redistribution of electrons in six potential wells located along [100] equivalent orientations in momentum space when stress is imparted to the material. Kanda in [8] presents the relation between the phenomenological and solid-state descriptions of this effect, as well as theoretical predictions for piezoresistive changes with temperature and doping concentration. These are presented in the form of a piezoresistive factor, $P(N,T)$, that appropriately scales the room temperature piezoresistive coefficient (see Figure 1). While this formulation is less accurate for large doping concentrations, the trends for both carrier concentration and temperature are valid and conceptually extensible to the effects of photoexcitation. The resultant increase in the total carrier concentration from excited carriers and the aforementioned steady-state temperature changes can both be expected to alter the piezoresistive coefficient.

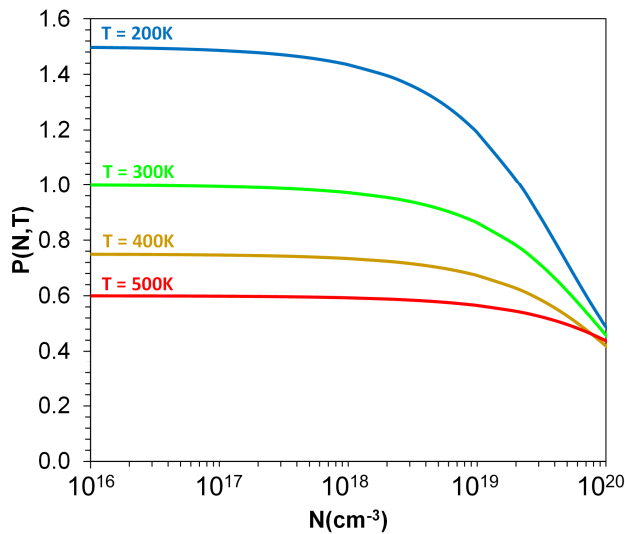


Figure 1: The adjusted piezoresistance factor $P(N,T)$ for n-type silicon as a function of carrier concentration and temperature, after Kanda [8]. The additional carrier concentration from photoexcitation adds to the dopant concentration (assumed fully ionized) in this model.

The impact of any reduction of the piezoresistive coefficient would be a proportional degradation of the magnitude of the motional conductance. Ultimately, this would result in shutoff of the self-sustained oscillation when the $R_{Agm} \leq -1$ gain condition required, as described in [4], is not satisfied;

with R_A being the resistance of the actuator arm.

EXPERIMENTAL METHOD

The experimental testbed used for this work is shown in Figure 2 and was identical to that used in previous work [5] for identifying the frequency of mechanical oscillation in ambient air. The applied DC bias voltage to the devices was first fixed to a value above the threshold needed to initiate self-sustained oscillation. This was verified by measuring the AC voltage output in the time-domain using a digital oscilloscope (Agilent DSO7032A, DC coupled, 1 M Ω input impedance). The HeNe laser was then attenuated by a filter wheel to a low power (≤ 1.21 mW) and positioned at the center of one of the outer plate edges. The photodiode captures the light reflected off of the underlying substrate and the device surface. The mechanical motion of the device structure modulates the intensity of this reflected laser return at the frequency of oscillation. A spectrum analyzer (Agilent 9320B) measured and recorded the corresponding electrical output of the photodiode. Once the device was verified to be functioning under low laser illumination, the electrical and mechanical (optical) responses were then measured as the laser power was incrementally increased using a filter wheel. Device operation was presumed to be in steady-state with measurements collected after several minutes for a given condition. The applied laser power for each filter wheel setting was measured after the experiment using a calibrated optical power meter at the output of the final objective lens.

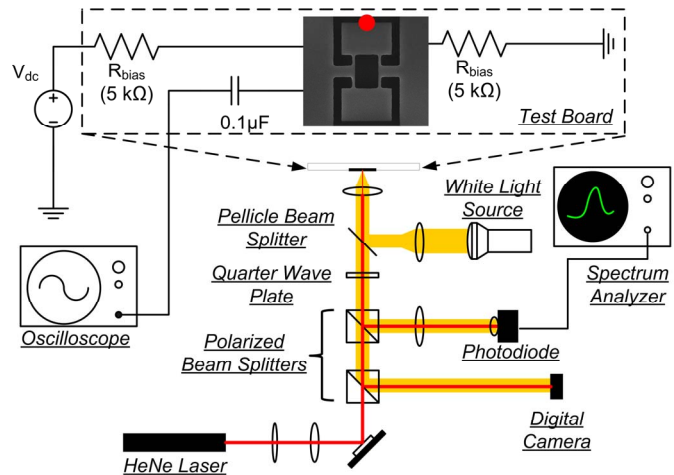


Figure 2: Optical testbed (ambient air, room temperature, ambient lighting) used for sensing the spectral response of the structural mode while measuring electrical output of the device in self-sustained oscillation. The filter wheel used to control laser power (not shown) is positioned prior to the beam splitters. (Position of laser shown on inset SEM image)

RESULTS AND DISCUSSION

Two central effects of increasing the laser power

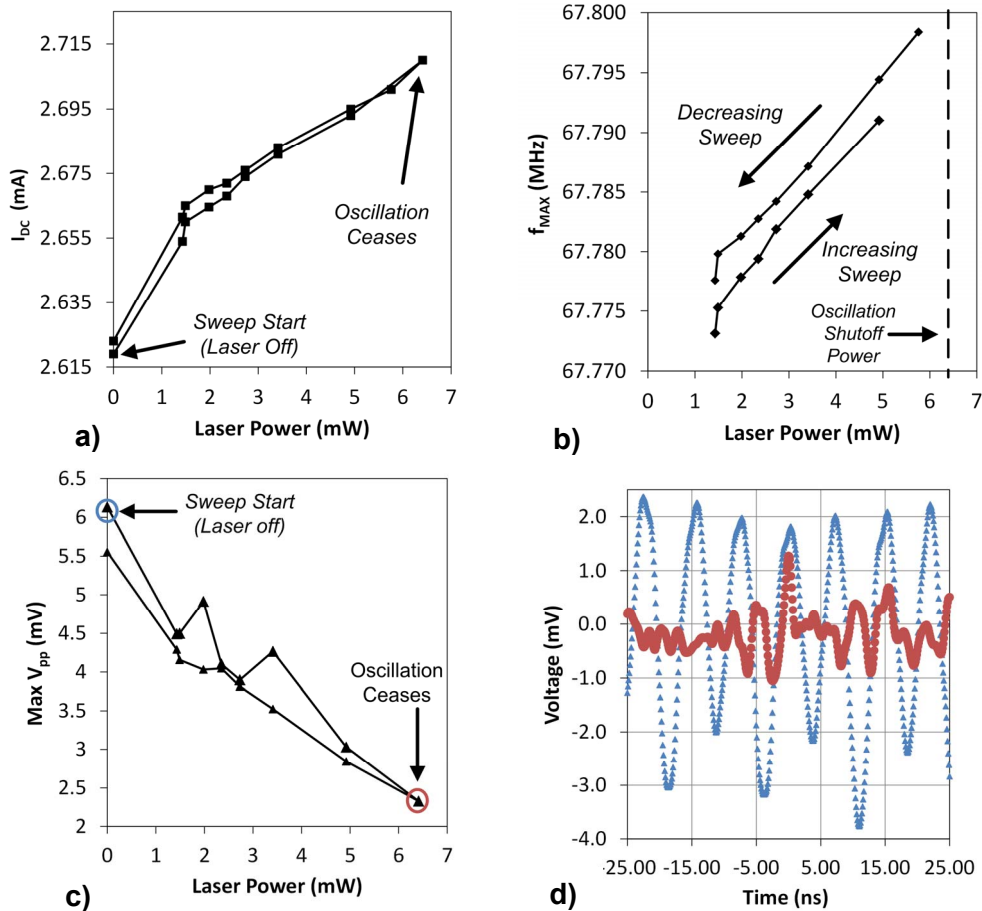


Figure 3: Steady-state experimental results for bi-directional laser power sweep of Device C6 under ambient air test conditions, $V_{dc} = 31.61 V$ (a) DC Current as measured by multimeter (b) Peak frequency of oscillation from 1D Lorentzian fit to photodiode output signal measured by spectrum analyzer (c) Maximum peak voltage difference of AC output signal as measured by digital oscilloscope d) Raw oscilloscope traces corresponding to initial laser off signal, and under shutoff illumination.

with the beam position fixed at a plate edge were observed for Devices C6 and A3 during experiment conduct. First, gradual degradation in the output signal strength and eventually complete quenching of the self-sustained oscillation, both electrically and mechanically occurred. Upon lowering the laser power back below this shutoff power level the self-sustained oscillation was restored. Second, increasing the laser power level caused increases in both the DC current and the frequency of device oscillation although this effect was not consistently linear for both devices at higher laser powers.

Experimental results for a bi-directional sweep of laser power up to a level beyond shutoff and back down to the initial test condition (laser off) are shown for Device C6 in Figures 3a-d). The frequency of oscillation shown in Figure 3b) is from fitting a 1D Lorentzian profile, as shown in [5], to the photodiode signal measured by the spectrum analyzer. The maximum raw peak-peak voltage observed in the electrical signal throughout the sweep is shown in Figure 3c), to depict the degradation in signal strength.

The variation of I_{DC} and peak frequency of oscillation, f_{MAX} , shown in Figure 3a-b) is consistent with considering the device as a self-oscillating photoresistor wired with bias resistors as shown in Figure 2. The photoexcitation of carriers lowers device resistance, which in turn decreases the DC power dissipation in the device, lowering the operating temperature, which stiffens the Young's modulus and ultimately causes an increase in frequency of oscillation. For comparison, the experimentally measured variation of I_{DC} and f_{MAX} results for Device A3 are shown in Figure 4 with a uni-directional (increasing) laser power sweep up to oscillation shutoff. It is clear that both I_{DC} and f_{MAX} reach a maximum and then decrease before oscillation shutoff. Since the laser was positioned approximately $\sim 1.5\mu m$ closer to the actuator arms for Device A3 than Device C6 the actual effective laser fluence on the actuator arms is higher. Thus the max peaks observed are likely due to the saturation limit of carrier excitation being reached in the actuator arms allowing scattering loss mechanisms to dominate and cause

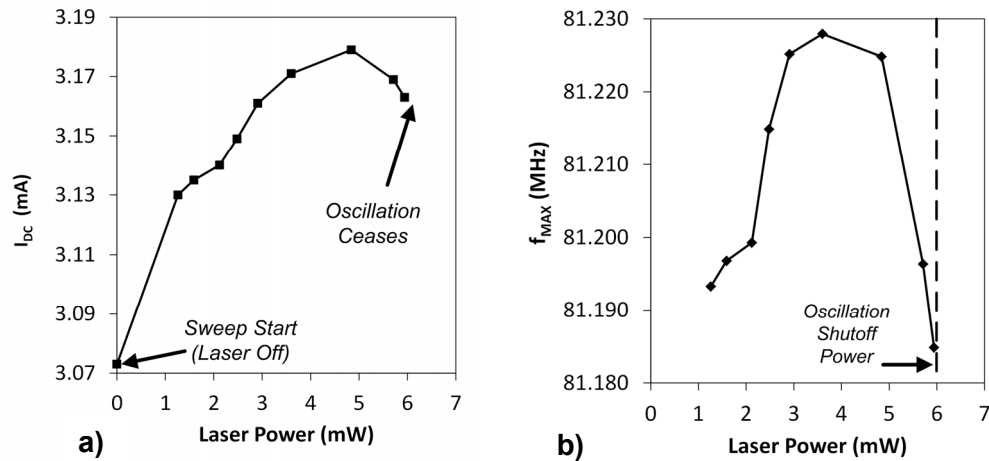


Figure 4: Steady-state experimental results for an increasing laser power sweep of Device A3 under ambient air test conditions, $V_{dc} = 37.96 V$ (a) DC Current as measured by multimeter (b) Peak frequency of oscillation from 1D Lorentzian fit to photodiode output signal measured by spectrum analyzer. The b dimension of Device A3 is $\sim 1.5 \mu m$ smaller than Device C6, thus the actual laser fluence on the actuator arms is higher than that for C6 for the same diameter laser spot.

an increase in electrical resistance.

It was also observed that positioning the laser at a low power setting closer to the actuation arms tended to degrade the electrical output in a similar fashion to that seen with measured data at the outer edge position, with quenching of the electrical output also possible. This observation supports the theory that the oscillation shutoff behavior observed is attributed to the piezoresistive coefficient and not an artifact of thermoelastic effects.

CONCLUSIONS

This work demonstrates thermal-piezoresistive oscillators can be frequency tuned and controllably quenched using continuous wave HeNe illumination of the structure. Such on/off control is believed to be novel to this class of device as it is predicated upon direct influence of the piezoresistivity of the material. This method of control potentially offers a unique way of integrating these devices with on-chip photonic circuitry. In addition, it invites further study of the effects of photoillumination upon the piezoresistivity of materials, which is an area that seems to be largely unexplored even for silicon. Formalizing more refined theory in this regard and further examining the modulation of piezoresistivity remain topics for future work.

ACKNOWLEDGEMENTS

The authors would like to thank Timothy May of the Integrated Teaching and Learning Laboratory and the Bunch Lab at CU Boulder for equipment support. Special thanks goes to Dr. Catalin Badescu of AFRL for discussions regarding the treatment of photoexcitation on piezoresistance. Additional thanks goes to Jason Gray and Joseph Brown of the Bright group for useful discussion and support. The lead author would like to acknowledge the DoD SMART Scholarship program for financial support.

REFERENCES

- [1] B. Dong, H. Cai, J. M. Tsai, P. Kropelnicki, A. B. Randles, M. Tang, D. L. Kwong, and A. Q. Liu, "NEMS actuator driven by optical gradient force," in *Transducers '13*, June 16-20 2013, pp. 900–903.
- [2] T. Kippenberg and K. Vahala, "Cavity optomechanics," *Opt. Express*, vol. 15, no. 25, pp. 74–77, 2007.
- [3] S. Sridaran and S. A. Bhavé, "Electrostatic actuation of silicon optomechanical resonators," *Optics Express*, vol. 19, no. 10, pp. 9020–6, May 2011.
- [4] A. Rahafrooz and S. Pourkamali, "Thermal-Piezoresistive Energy Pumps in Micromechanical Resonant Structures," *IEEE Trans. Electron Devices*, vol. 59, no. 12, pp. 3587–3593, Dec. 2012.
- [5] H. J. Hall, D. E. Walker, L. Wang, R. C. Fitch, J. S. Bunch, S. Pourkamali, and V. M. Bright, "Mode selection behavior of VHF thermal-piezoresistive self-sustained oscillators," in *Transducers '13*, June 16-20 2013, pp. 1392–1395.
- [6] A. Rahafrooz and S. Pourkamali, "High-Frequency Thermally Actuated Electromechanical Resonators With Piezoresistive Readout," *IEEE Trans. Electron Devices*, vol. 58, no. 4, pp. 1205–1214, 2011.
- [7] W. P. Mason, *Physical Acoustics*. New York: Academic Press, 1964, pp. 183–190.
- [8] Y. Kanda, "A graphical representation of the piezoresistance coefficients in silicon," *IEEE Trans. Electron Devices*, vol. 29, no. 1, pp. 64–70, Jan. 1982.

CONTACT

*H.J. Hall, Tel: +1-303-492-7151; Email: Harris.Hall@colorado.edu